Revisiting the Structure of $(LiCH_3)_n$ Aggregates Using Car−Parrinello Molecular Dynamics

Hélène Gérard,*,† Aurélien de la Lande,† Jacques Maddaluno,‡ Olivier Parisel,† and Mark E. Tuckerman§

Université Pierre et Marie Curie − Paris 6, Laboratoire de Chimie Théorique, UMR 7616, CC 137, 4 place Jussieu, 75252 Paris Cedex 05, France, CNRS, UMR 7616, 75005 Paris, France, Laboratoire des Fonctions Azotées & Oxygénées Complexes de l'IRCOF, UMR 6014 CNRS, Université de Rouen, 76821 Mont-Saint-Aignan Cedex, France, and Department of Chemistry and Courant Institute of Mathematical Sciences, New York University, 100 Washington Square East, New York, New York 10003

Received: November 2, 2005; In Final Form: February 7, 2006

The theoretical study of $(LiMe)_n$ aggregates using Car−Parrinello molecular dynamics was undertaken. With respect to a quantum chemical static treatment, this approach furnishes supplementary information about the structural parameters. Equilibrium structures are indeed stable to ca. 300 K, provided the methyl groups in the aggregates are considered to rotate essentially freely. The Li−C distance depends on the coordination number of Li and not so much on the degree of aggregation. Finally, above 650 K, the cubic $LiCH_3$ tetramer (which is energetically favored) undergoes an entropy-driven rearrangement to a planar structure.

Introduction

Modern quantum chemical methods have proven their ability to describe the structure and reactivity of many kinds of systems of chemical interest. In particular, density functional theory (DFT) calculations have enlarged the field of theoretical applications by successfully encompassing more realistic entities and chemically relevant environments. Microscopic phenomena such as the solvation, the chemical selectivity, or the asymmetric induction, for instance, have become accessible to theory because of the relatively low computational overhead of the DFT approach. However, standard quantum chemistry techniques only provide a static description of a system that is useful when the usual hypotheses are valid, that is, when the potential energy surfaces (PES) exhibit a small number of well-defined and deep minima. These conditions are seldom met when the number of degrees of freedom increases or when the PES are shallow. Therefore, static methods are de facto limited for systems exhibiting a large number of conformers. Classical molecular dynamics (MD), which includes conformational sampling, offers an alternative solution to the static approach. However, MD generally uses molecular mechanics and thus depends on the availability and reliability of adequate parametrizations. More recently, parameter-free ab initio molecular dynamics (AIMD) methods have been introduced and have become increasingly popular. By allowing both conformational sampling (on a time scale of a few picoseconds) and bond breaking and formation, AIMD calculations are expected to be well-adapted to the investigation of systems of chemical interest. Some insightful examples in the field of lithium chemistry can be found in the literature.[1−7] All of these indicate the importance of thermal effects on the time scale of the simulations. This is especially noteworthy in the case of metallic lithium clusters, which are known to exhibit high structural flexibility.[1−3] For these clusters, AIMD was used to complement static studies and proved that thermal fluctuations have "sizable consequences at experimentally relevant temperature".[3] In particular, these studies were used to propose new structural isomers and to investigate the mechanism of pseudorotations observed experimentally. AIMD was also used to investigate the solvation of the Li^+ cation in water.[4,5] A well-defined four-water solvation shell was found, and the residence time of water molecules within this shell was found to lie within a 20−50 ps range. Other studies in the field of organolithium compound structure and chemistry have also appeared. A structural study of C_2H_2-Li_2 using AIMD showed the capability of simulated annealing to provide a variety of equilibrium structures, among which hydride-containing isomers were proposed as kinetically relevant intermediates.[6] In another study, mechanistic insights in the anionic polymerization process using constrained dynamics were described.[7]

In this context, alkyllithium compounds $C_nH_{2n+1}Li$ present remarkable challenges for such studies. Experimental investigations on these species have shown their tendency to form aggregates either in solution[8] or in the gas phase.[9] Numerous spectroscopic and reactivity data evidence the dynamic behavior of these species. We also note the temperature dependence of the NMR spectrum of $(MeLi)_4$,[10−13] the importance taken by dynamic phenomena in organolithium spectroscopy,[14−19] the fast racemization of asymmetric alkyllithium,[20−23] or the complex fragmentation schemes involving $(MeLi)_4$ elaborated to interpret mass spectroscopy measurements.[9] Extensive static theoretical studies on these compounds have furnished a large amount of information about their microscopic structures and reactivity: (i) numerous isomers were localized for the most commonly studied aggregates (dimer, tetramer, etc.),[24−26] while energetic and spectroscopic properties were computed and favorably compared to experimental results,[27−29] (ii) reaction paths were proposed for organic reactions,[30,31] and (iii) the impact of solvation on these processes was examined and was shown to play an important role.[32] There is thus a clear scientific interest in applying AIMD to these species, because most processes of

* Corresponding author. Tel.: (33) 144 279 662. Fax: (33) 144 274 117. E-mail: helene.gerard@lct.jussieu.fr.
† Université Pierre et Marie Curie and CNRS.
‡ Université de Rouen.
§ New York University.

10.1021/jp056326h CCC: $33.50
Published on Web 03/17/2006

experimental interest take place with low-energy barriers that can be surmounted on the time of present-day simulations. In fact, the extremely reactive organolithium compounds are associated with very short-lived intermediates that are, in general,[33−35] not accessible to spectroscopic monitoring. Additionally, most kinetically relevant phenomena exhibit associative or dissociative mechanisms for which molecular dynamics methods are required to properly account for entropic contributions.

In this paper, we present a Car−Parrinello (CP) molecular dynamics study,[36] which aims at evaluating the impact of thermal fluctuations and conformational flexibility on the structural properties of model organolithium aggregates. A validation of the level of theory is first proposed using the prototype inorganic $(LiX)_n$ clusters (X = Cl and Br, $n = 1-4$), and the dynamic results are compared to previous static results. Finite-temperature simulations of various MeLi oligomers at 300 K are then reported. Finally, the behavior of the MeLi tetramer at higher temperatures (600 and 800 K) is presented.

Results and Discussion

Validation of Computational Protocol. *Computational Details.* Static ab initio computations were carried out using the Gaussian 03 suite of programs,[37] using the BLYP[38] and B3P86[39] functionals with the 6-31+G** or the 6-311++G(2d,2p) basis sets. The nature of each optimized minimum was checked using frequency computations performed within the harmonic approximation. No scaling procedure was applied. For CP molecular dynamics calculations, the PINY-MD program was chosen,[40] using the BLYP functional, a plane wave (PW) basis set, and Goedecker[41] (Li) and Troullier−Martins[42] (other atoms) pseudopotentials; this approach will thereafter be referred to as BLYP/PW. We employed the cluster boundary condition method of Martyna and Tuckerman[43] and a plane-wave energy cutoff (E_{cut}) of 80 Ry. Both E_{cut} and the box sizes were adjusted for each system to yield energies converged to chemical accuracy. CP simulations were carried out at constant temperature using Nosé−Hoover chains of length 4 on the atoms.[44] It was checked that the fictitious electron kinetic energy remained small compared to that of the nuclei (adiabaticity) without need for electronic thermostating (using $\mu = 680$ amu). In all simulations, the time-step was 0.125 fs. The total simulation time was about 10 ps for each species studied except for the planar form of Li_4Me_4 as well as Li_6Me_6 for which the simulation time was 5 ps.

Comparison to the Static Results. The influence of the level of theory is first studied for LiCl. The PES as obtained from the various methods is described as $\Delta E_{meth}(x)$, computed as the energy difference between the energy for a given distance x (labeled $E_{meth}(x)$) and that at the minimum ($x_{meth}°$), that is, $\Delta E_{meth}(x) = E_{meth}(x) - E_{meth}(x_{meth}°)$. The PESs using various methods are very similar: the largest discrepancy is found to be around 10%. Consequently, the comparison is enhanced by plotting $\Delta(\Delta E)_{meth}(x) = \Delta E_{meth}(x) - \Delta E_{ref}(x)$, that is, the difference between the PES for a given method and that for the reference method, the BLYP/PW result. These values are plotted in Figure 1 for large and small displacements around the equilibrium position (2.03 Å). The discrepancies that appear at both the BLYP/6-31+G** and the B3P86/6-31+G** levels are mostly due to the small basis set used. It is nevertheless important to note that a nearly perfect fit is obtained between the BLYP/6-311++G(2d,2p) approach and the reference BLYP/PW calculations. This result shows that the PW basis/pseudopotential approach yields results equivalent to a high-quality Gaussian basis set. This excellent agreement, found for large and small displacements, ensures that the CP dynamics calculations are reliable for distortions of any amplitude for the species to be investigated.

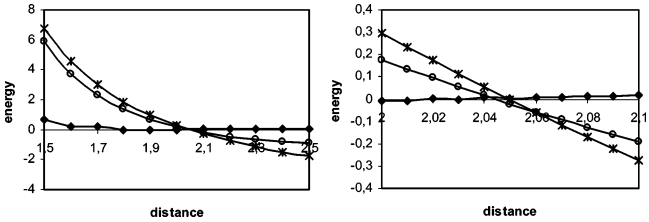

Figure 1. $\Delta(\Delta E)_{meth}$ (see text for details) for long (left) and short (right) range variations of the Li−Cl bond in LiCl. Distances are in Å, and energies are in kcal mol^{-1}. Diamond (BLYP/6311++G(2d,2p)); stars (BLYP/6-31+G**); circles (B3P86/6-31+G**).

TABLE 1: Aggregation Energies (AE, See Text for Definition, in kcal mol^{-1}) of the $(LiCl)_2$ Aggregates and Geometrical Parameters (in Å)

	Li···Cl	Li···Li	Cl···Cl	AE
B3P86/6-31+G**	2.225	2.637	3.587	49.8
BLYP/6-31+G**	2.240	2.621	3.634	47.8
BLYP/6-311+G(2d,2p)	2.210	2.559	3.645	47.0
BLYP/PW	2.219	2.600	3.597	48.0

The structure and energetics of $(LiCl)_2$ at its equilibrium geometry were studied next, and the results are reported in Table 1. As for the monomer, no major effect of the method or of the basis set was found; good agreement for the Li−Cl distance is obtained between both BLYP/6-31+G** and B3P86/6-31+G**, which compares two functionals for the same basis set, and between the BLYP/6-311++G(2d,2p) and the BLYP/PW basis sets, which compares two basis sets for the same functional. Slightly larger discrepancies are observed for the Li−Li and Cl−Cl distances. The corresponding aggregation energy (AE), defined as the difference between the energy of the optimized aggregate and that of the optimized monomers, varies within 2 kcal mol^{-1}, depending on the functional, and within 1 kcal mol^{-1} depending on the basis set. It thus appears that no major effect due to the functional or to the basis is expected for this dimer, the energy differences being within chemical accuracy.

It can be expected that the BLYP/PW methodology provides results of similar accuracy for systems differing either by the state of aggregation or by the nature of the anion. Indeed, previous studies have shown that the higher the aggregation state the less sensitive are the results to the computational methodology.[32,45] This is a likely consequence of the fact that the electronic densities of highly under-coordinated species are difficult to obtain accurately. Despite the strong ionicity of the LiCl bond,[46−48] the BLYP/PW descriptions of the energies and the geometrical parameters are satisfactory. It follows that BLYP/PW was retained to study $LiCH_3$ and LiBr.

Motion of Inorganic Aggregates. Because the aggregate is studied in the gas phase, and thus in the absence of solvent or other external ligand, its structure is likely to fluctuate around the geometry of the minimum. Consequently, a dynamical simulation starting from the optimized structure of an aggregate is expected to remain in the vicinity of the starting point and to yield average parameters similar to the optimized ones. This hypothesis is tested in this section to evaluate the relevance of the method in the study of the four $(LiX)_n$ structures described in Figure 2 for X = Cl.

We first discuss the different ways of classifying the $(LiX)_n$ aggregates. Two different descriptions have been proposed. The first one is based on the coordination number of the Li atom, n_c. Note that species differing by their aggregation level (n)

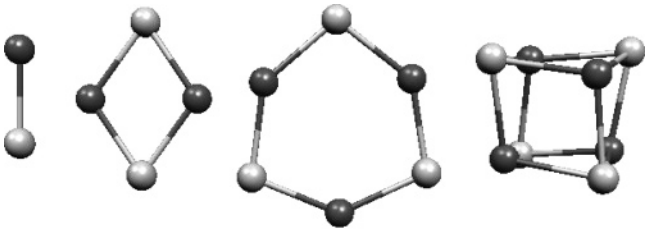

Figure 2. Structure of the $(LiCl)_n$ aggregates ($n = 1-4$).

TABLE 2: Distances and Angles for Geometries Optimized (Opt) or Averaged (Av) along the Simulation Time and Corresponding rmsd[a]

	LiCl			LiBr		
	Opt	Av	rmsd	Opt	Av	rmsd
			Li−X			
$n = 1$	2.032	2.046	0.059	2.190	2.195	0.070
$n = 2$	2.210	2.234	0.091	2.379	2.390	0.096
$n = 3$	2.196	2.218	0.087	2.363	2.376	0.094
$n = 4$	2.332	2.370	0.130	2.509	2.541	0.162
			X−X			
$n = 2$	3.605	3.617	0.097	3.939	3.935	0.110
$n = 3$	4.160	4.131	0.162	4.527	4.470	0.167
$n = 4$	3.646	3.687	0.124	3.963	3.999	0.151
			Li−Li			
$n = 2$	2.559	2.598	0.120	2.668	2.681	0.135
$n = 3$	3.298	3.324	0.233	3.438	3.409	0.265
$n = 4$	2.855	2.912	0.161	3.003	3.044	0.189
			Li−X−Li			
$n = 2$	70.7	71.1	3.7	68.2	62.7	3.1
$n = 3$	97.4	97.5	8.9	93.4	93.4	9.0
$n = 4$	75.4	75.8	4.7	73.5	73.6	5.1
			X−Li−Li−X			
$n = 2$	180.0	181.0	9.9	180.0	179.3	10.8
$n = 3$	180.0	180.5	16.4	180.0	178.7	16.7
$n = 4$	197.5	197.0	6.3	199.4	199.4	7.1

[a] Distances are given in Å, and angles are in deg.

can be characterized by the same coordination number: $n_c = 1$ for $n = 1$, $n_c = 2$ for $n = 2$ and 3, and $n_c = 3$ for $n = 4$. The second classification scheme used is based on the ligand close-packing model,[49] which assumes that the anions are in close contact and determine the molecular geometry. This arrangement leads to the shortest possible X···X distance. The data in Table 2 show that the dimer and the tetramer are close-packed structures whereas the cyclic trimer is not. The value of 3.62 Å for the Cl···Cl interaction in these Li clusters is in line with the average Cl···Cl distances found for chlorinated beryllium, boron, and carbon derivatives.[50]

Simulations of the aggregates in the gas phase were carried out for approximately 10 ps. As expected, whatever the value of n or the nature of X (X = Cl or Br), no major rearrangement of the starting structure was observed. The main geometrical parameters and their root-mean-square deviations (rmsd) are reported in Table 2, together with the static values.

The average distance value is very similar to that obtained from static studies, the discrepancy being less than 0.06 Å and always smaller than the rmsd, which confirms the accuracy of the method. Structural parameters can thus be derived by averaging the distances over the trajectory. No systematic trends are observed, but the average Li−X distances are slightly longer than the static ones due to anharmonic effects. Additionally, the differences between the static minimum and the thermal average value tend to be larger for the Li−Li or X−X distances than for the Li−X ones.

Additional information on the structural properties can be obtained from the rmsd. A simple rule stating that "the longer the bond, the larger the rmsd" can be assumed, but significant departures from this rule can also be observed in some specific cases (depending both of X and n). Such counterintuitive behavior can be considered as yielding vital insights in the dynamic properties of the system.

As it turns out, the Li−X averaged bond lengths and rmsd increase not with n but with the coordination number n_c: the higher the value of n_c, the longer the Li−X bonds and the wider the distributions. In particular, the parameters for the two structures with $n_c = 2$ ($n = 2$ and 3) are similar. In contrast, the X−X distributions do not follow this trend: the averaged distances are short, and the rmsd is small for $n = 2$ and 4. Both values are much larger for $n = 3$. In fact, the values for both $(LiX)_2$ and $(LiX)_4$ are characteristic of close-packed X^- anions:[50] the X−X lengths average within 0.07 Å, while the Li−X bond lengthens by more than 0.14 Å between $(LiX)_2$ and $(LiX)_4$. On the other hand, the X−X length distributions in $(LiX)_3$ are much larger than they are in the two previously mentioned species and thus too large for a X−X contact. They are also significantly shorter than those obtained from static quantum chemistry calculations. The corresponding rmsd values are much larger than those of the close-packed structures (0.165 and 0.167 Å for X = Cl and Br, respectively), but they are similar for Cl and Br, independent of the X···X distances. All these points support the variability of the X···X distance as they relate to the close-packed nature of the aggregate and not to the coordination number of Li. In contrast, the Li···X distance was consistently found to be connected to n_c. The behavior of the Li−Li distance derives from these two sometimes-competing tendencies, which makes the analysis difficult. It should be noted that both the distance and the rmsd increase in the following order: dimer < tetramer < trimer.

The geometrical arrangement around the X substituent is characterized by the distributions of the Li−X−Li angles. The AIMD-averaged and static data are consistent with one another. Their rmsd values vary monotonically with their average. The X−Li−Li−X dihedral angles show that both the dimer and the trimer are planar, whereas the faces of the cubic tetramer slightly depart from planarity. A large rmsd is found for $(LiX)_3$, providing evidence of large amplitude out-of-plane motion in the trimer, not observed in the dimer or the tetramer.

The geometrical parameters characterizing the clusters thus exhibit a dual behavior related to the two structural properties described above. The coordination number of the Li atoms drives the length and the floppiness of the Li−X bonds. The close-packing of the anions determines the average and the rmsd of the X−X distances, as well as the out-of-plane fluxionality, and thus the general dynamical profile of the aggregates. It is noteworthy that AIMD provides access to quantitative parameters not available from static calculations such as the rmsd and the difference between the static and average values. In particular, the rmsd evaluates the floppiness of a single geometrical parameter and therefore can be used to build a scale of flexibility.

Structural Properties of Organic Aggregates. We next moved to the application of the dynamical methods validated above to organolithium compounds. These compounds are key reagents in organic synthesis, and their structure has been widely investigated, both in the gas phase and in solution. For instance,

TABLE 3: BLYP/6-311++G(2d,2p) Aggregation Energies Per MeLi Units in kcal mol^{-1}[a]

n	2	3	4 cube	4 plane	6
n_c	2	2	3	2	3
LiMe	20.5	26.4	30.1	27.6	31.9
	(14.7)	(19.1)	(20.3)	(19.6)	(21.0)

[a] Free energies computed within the harmonic approximation are given in parentheses.

the canonical monomeric MeLi has been widely studied[51] in the gas phase[52−54] and has been shown to crystallize as strongly interacting $(MeLi)_4$ units.[55,56] Substantial NMR data on alkyllithium in various solvents are available and have led to the conclusion that the level of aggregation depends mainly on the nature of the solvent and on the steric hindrance of the alkyl chain. For example, in noncoordinating solvents such as cyclopentane and toluene, tetramers and hexamers are both encountered for nonfunctionalized alkyl derivatives. In the following, MeLi was retained as a model alkyllithium compound, and aggregation levels up to the hexamer were considered. Note that no solvation was taken into account at this level. This AIMD study will thus serve to complement the numerous static theoretical studies,[24−32,45−48] providing deeper insight into the fluxional behavior of MeLi aggregates.

Static and Average Parameters of the $(MeLi)_n$ Backbone. Monomeric MeLi and several of its aggregates were studied. We first report on the static calculations. Only one structure could be optimized for the dimer, the trimer, and the hexamer, even though ladder structures were considered as starting points for the latter two compounds. The trimer is a planar crown with alternate Me and Li similar to that described in Figure 2 for $(LiCl)_3$. The hexamer can be described as an assembly of two trimers stacked one on top of the other. There are thus two types of "short" Li−C distances, one within a trimer crown (intratrimer distance), and another one between the crowns (intertrimer). The same comment applies to the other geometrical parameters. Two structures can be found for the tetramer. One is the canonical cubic $(MeLi)_4$, whereas the other is a planar square.

The energy values for aggregation (Table 3) for the dimer and tetramer fall within the limits found in the literature (19.5−23.6 kcal mol^{-1} for the dimer and 29.1−32.9 kcal mol^{-1} for the tetramer),[26] the higher is the aggregation level, the more stable the complex. It is nevertheless noteworthy that, except for the dimer, aggregates with identical n_c but different n values exhibit similar energies. Thus, n_c seems to be a leading factor in the aggregation energy per monomer. In the absence of solvent, the hexamer remains the most stable species. Nevertheless, the energy difference with the cubic tetramer is small, and the stability order can thus be reversed by changes of the alkyl chain,[26] in agreement with the experimental data.[10] For instance, it is known from $^1J(^{13}C-^6Li)$ NMR measurements that ^{t}BuLi exists as a tetramer in cyclopentane whereas ^{n}PrLi forms hexamers in the same solvent. ^{s}BuLi and secondary pentyllithium even exist under both aggregation states in this apolar noncoordinating solvent.[10]

Additionally, each aggregate is more stable than its lower sized fragments so that all of these systems can be treated dynamically without expecting any dissociation at 300 K, as shown from the free energy values (Table 3). However, a rearrangement of the metastable planar tetramer to its cubic isomer is possible if not hindered by high-energy barriers.

Next, AIMD simulations were carried out on these aggregates. Whatever the value of n and the starting geometry, no major rearrangement of the structure was observed. This is not in contradiction with the well-known dynamic behavior of the alkyllithium observed by NMR spectroscopy[10,11,57] although the time scale for CP simulations is about 10^6 time shorter than that of NMR probing. In particular, the planar tetramer is not converted to a cube within the simulation time: the activation barrier for this transformation is too high to be overcome within time of simulation, indicative of energies larger than 2 kcal mol^{-1}, consistent with the literature results.[31]

Averages of the main structural parameters, together with the associated rmsd, have been evaluated (Table 4). Differences between the averaged values and the optimized ones (not reported) remain very small as compared to the rmsd.

As in the case of the halogenated compounds, Li−C distances and rmsd increase with n_c, so that rmsd values are found to be linearly correlated to the Li−C distances. A much less intuitive behavior is observed for the C−C distances. Two groups of distances are found, depending on the compactness of the aggregates. The dimer and the cubic tetramer have short C−C distances, consistent with contacts between the anions, whereas C−C distances are much longer for the trimer and the planar form of the tetramer. Interestingly, these two features are observed in the hexamer, whereas the C−C distances are long within a trimer and much shorter between the trimers, in direct contrast with the Li−C distances. As shown earlier, the trimer is a floppy species and retains this characteristic within the hexamer, whereas the stacking of the two trimers is a compact interaction with close contact of the Me entities. On the other hand, the rmsd's do not follow this compact/floppy classification, so that rmsd's and distances cannot be correlated. The C−C rmsd increases with n_c in the compact aggregates and is equal to the rmsd of the Li−C interactions. For the Li−Li distances, the rmsd is also found to be linearily correlated with the corresponding distances, which are shorter for compact aggregates (dimer and cubic tetramer) and longer for the noncompact ones. It is noteworthy that, for compact aggregates, the Li−C, Li−Li, and C−C rmsds are equal so that all distances

TABLE 4: Distances and Angles Averaged along the Simulation Time (rmsd in Brackets)[a]

	Li−C	Li−Li	C−C	C−Li−Li−C	Li−C−Li
$n = 1$	1.988 [0.070]	NC[b]	NC	NC	NC
$n = 2$	2.120 [0.099]	2.206 [0.094]	3.603 [0.093]	180.1 [10.2]	62.6 [3.1]
$n = 3$	2.092 [0.094]	2.677 [0.152]	4.069 [0.129]	179.8 [17.0]	79.6 [5.4]
	3.881 [0.189]				
$n = 4$ cubic	2.232 [0.126]	2.449 [0.123]	3.625 [0.130]	206.0 [6.9]	66.5 [3.9]
($n_c = 3$)	3.717 [0.128]				
$n = 4$ planar	2.078 [0.087]	2.824 [0.167]	4.093 [0.122]	178.1 [21.7]	85.7 [6.3]
($n_c = 2$)	4.435 [0.275]				
$n = 6$ ($n_c = 3$)					
intratrimer	2.19 [0.114]	3.03 [0.200]	4.10 [0.183]	211.2 [9.7]	87.5 [7.0]
intertrimer	2.31 [0.159]	2.47 [0.132]	3.59 [0.146]	213.5 [7.3]	NC

[a] Distances are given in Å, and angles are in deg. [b] NC stands for Not Concerned.

TABLE 5: Optimized (Opt), Average (Av), and rmsd Values for the H−H−C−H Dihedral Angle in the CH_3 Moieties of the $(LiCH_3)_n$ Aggregates

	H−H−C−H[a]		
n	Opt	Av	rmsd
1	113.1	113.1	6.7
2	106.8	107.8	6.0
3	107.0	107.7	6.0
4 cube	106.6	106.1	5.8
4 plane	107.4	107.9	6.0
6	105.7	106.0	5.7

[a] Angles given in degrees.

exhibit similar fluctuations. Such behavior was not observed in the case of the halogenated aggregates and probably relates to particularly favorable inclusion of the Li^+ cation in the "holes" between the CH_3^- anions.

This difference in the motion between the compact and noncompact structures is especially meaningful in the case of the hexamer where the shortest C−C distances appear to be also the more fluxional. Consequently, motions inducing variations in the C−C distances will be entropically favored within a trimer but disfavored between trimers. This part of the study suggests that the rmsd can be considered as a complementary parameter to characterize molecular structures.

Motion of the CH_3 Entity. The next part is focused on the study of the motions of the CH_3 group within the $(LiMe)_n$ aggregates: the rearrangements within the CH_3 moieties and the orientation of CH_3 with respect to the Li skeleton and to the other CH_3 moieties were considered successively.

We first examined the fluctuations of the shape of the CH_3 groups by computing and plotting the H−H−C−H angle versus simulation time for various aggregation states. These dihedral angles were found to evolve around a single value close to 110° ± 25. Two conclusions can be drawn from this observation. First, no inversion of the CH_3 moiety is observed during the time of the simulation, because such a rearrangement would imply a change in the sign of the H−H−C−H angle. This is in line with previous theoretical studies showing that the experimentally observed[20] inversion takes place with an activation barrier of about 20 kcal mol^{-1}.[31] Moreover, no major distortion of the CH_3 moiety occurs due to thermal effects; that is, the carbon atom remains tetrahedral. More detailed results are obtained by calculating average and rmsd values (Table 5). The average dihedral angle is much smaller than 120° and tends to decrease from 113° to 108° and 106° when the coordination number at Li increases from 1 to 2 to 3. Note that values for $n = 4$ (planar), $n = 3$, and $n = 2$ are equal (107.8° ± 6.0, $n_c = 2$) as well as values for $n = 4$ (cubic) and $n = 6$ (106.0° ± 5.8, $n_c = 3$). This is consistent with an angle value and a motion governed by the coordination number n_c. The rmsd also decrease with n_c: the CH_3 moiety is found to become less flexible as the coordination number increases. This might be related to the hyperconjugation in alkyllithium oligomers[24] restraining the motions of the CH_3.

Rotation of CH_3. Conformational fluctuations of the CH_3 group were investigated next. These conformations can be described with respect either to another CH_3 group or to the Li skeleton. Two dihedral angles are thus reported: (i) the H−C−C−H angle, which provides information about the relative orientation of a CH_3 moiety with respect to the others, and (ii) the H−H−Li−Li angle, which describes the orientation of a given H−H−H triangle with respect to the Li−Li−Li triangle it faces. This study was only undertaken for $n = 2$ and 4 (cubic) because the observed motion is slow and requires a long simulation time to ensure a proper sampling. These two angles, plotted as a function of the simulation time for $n = 2$ and 4, are shown in Figure 3. For all values of *n*, free rotation of the CH_3 group is observed. Yet, as far as the description of conformers is concerned, a very different behavior with *n* is obtained. For $n = 2$, the Me units do not adopt any preferred orientation, either with respect to other CH_3 units or with respect to the Li−Li axis. This is consistent with other static theoretical calculations.[26,31] By contrast, for $n = 4$, three positions are preferred and connected by fast interconversions. These positions correspond to 60°, 180°, and 300° for the H−H−Li−Li angle, and to 0°, 120°, and −120° for the H−C−C−H angles: the CH_3 units adopt an eclipsed arrangement with respect to each other, as well as with respect to the Li−Li−Li face of the tetrahedron directly across. This is confirmed by the structure given in Figure 3, obtained from a time average geometry over about 1 ps and centered at about $t = 8$ ps. The existence of a preferred conformation in the tetramer thus constitutes a fundamental difference from the dimer. The free energy barrier for the rotation of the CH_3 in the tetramer can be evaluated from the ratio of the probability distribution function (pdf) value at the maximum and the minimum of the curve because:

$$\mathrm{pdf(min)/pdf(max)} = \exp(-\Delta_r G^{\ddagger}/RT)$$

We obtain $\Delta_r G^{\ddagger}$ values of 1.0 kcal mol^{-1} with respect to another CH_3 and 1.5 kcal mol^{-1} with respect to the Li−Li−Li triangle directly underneath. These values are to be taken with caution because the simulation time for the $(LiMe)_4$ structure is too short to provide a complete sampling of these slow motions. Nevertheless, the barriers obtained are comparable to those found in the literature.[26]

Interconversion between the Two Tetrameric Structures. AIMD simulations of $(MeLi)_4$ provide evidence that the planar form is subject to larger thermal fluctuations than its cubic isomer. This can be understood in light of the thermodynamic data computed within the harmonic approximation on the optimized static structures. These values are reported in Table 6 for $T = 298$ K. It appears that the planar tetramer is electronically disfavored by more than 10 kcal mol^{-1}. Zero-point energy effects favor the planar structure by 2 kcal mol^{-1}, but these corrections are canceled by the thermal contributions to the internal energies *U*. The major thermal effects thus appear in the entropic contributions to the free energies *F*. Indeed, at 298 K, entropy favors the planar form by more than 24 cal mol^{-1} K^{-1}, which lowers the free energy preference for the cubic form to 2.8 kcal mol^{-1}. Consequently, at the simulation temperature, the planar structure should rearrange to a cubic structure, provided this rearrangement is not too slow. Previous static studies reported this barrier to be about 5 kcal mol^{-1} (from the plane to the cube), which justifies the absence of rearrangement.[31] Using these ΔU and ΔS values within the Ellingham approximation leads to $\Delta F = 0$ for $T_i = 412$ K. Above this inversion temperature, the planar tetramer becomes the most stable structure.

An AIMD simulation was then carried out on the cubic form of the tetramer at 600 and 800 K, where this structure is supposed to be disfavored by 4.6 and 9.5 kcal mol^{-1}, respectively, with respect to the planar isomer. Additionally, the rearrangements should be kinetically easier than at 300 K. It should be kept in mind that these are microscopic rovibrational temperatures that are not identified to the temperature of a full experimental sample.[58] This is a commonly used procedure to simulate, in these conditions, a local increase of internal energy.[6,59]

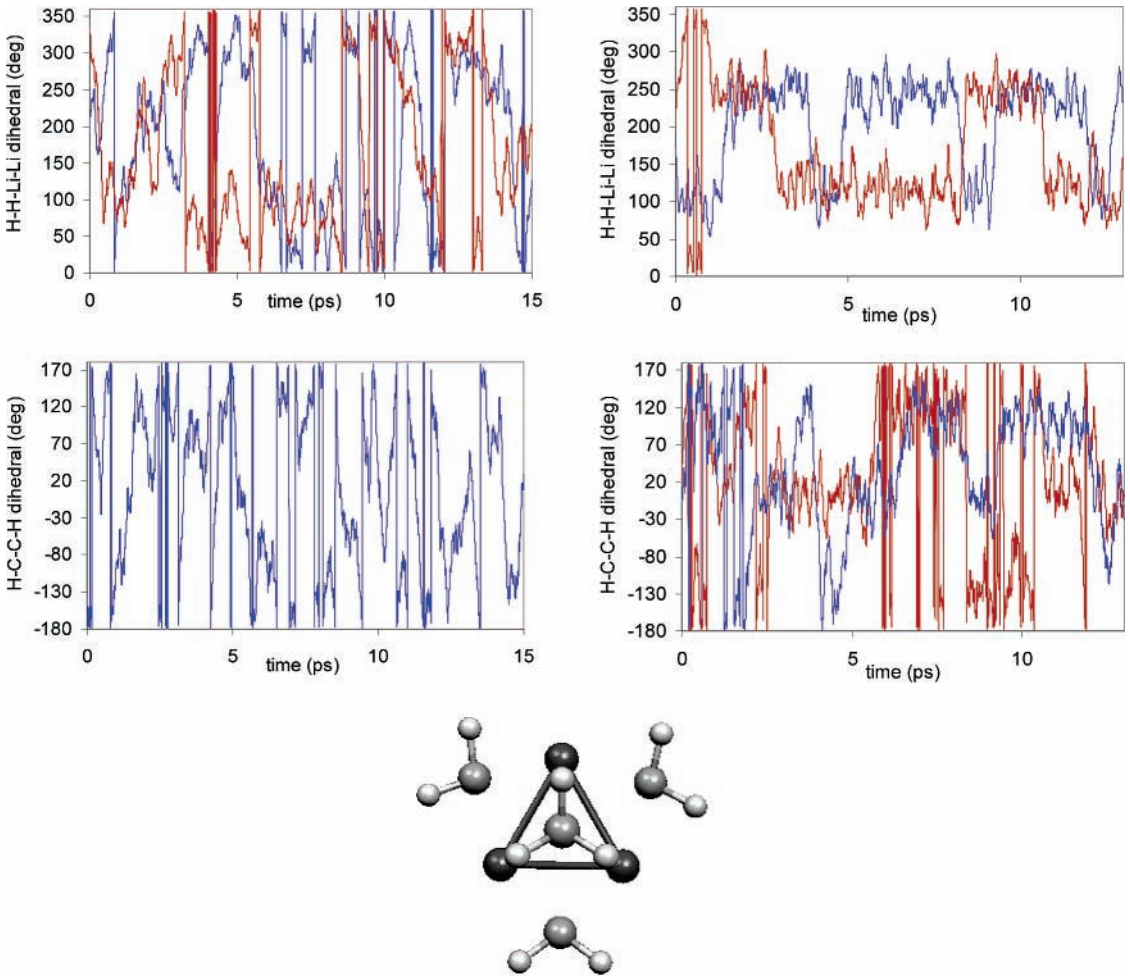

Figure 3. Orientation of the CH_3 group with respect to the skeleton (top, H−H−Li−Li dihedral angle in deg) and other CH_3 groups (bottom, H−C−C−H dihedral angle in deg) for Li_2Me_2 (left) and cubic Li_4Me_4 (center) as a function of time (ps) for a 300 K simulation. Average orientation of the CH_3 groups (bottom).

TABLE 6: Thermal Corrections to Li_4Me_4 Structures at 300 K

$\Delta(E°)$ (kcal mol^{-1})	10.4
$\Delta(E+\text{ZPE})$ (kcal mol^{-1})	8.3
ΔU (kcal mol^{-1})	10.1
ΔS (cal mol^{-1} K^{-1})	24.6
ΔF (kcal mol^{-1})	2.8

Unfortunately, no major rearrangement was observed at 600 K during the simulation (11 ps). However, a much larger rmsd (0.229 Å as compared to 0.126 Å at 300 K) as well as a significant lengthening (+0.06 Å leading to a distance of 2.292 Å as compared to 2.232 Å at 300 K) are computed for the Li−C bonding distances. Consequently, partial opening of the cube temporarily takes place during the course of simulation as shown in Figure 4. It appears that two opposite Li···C sides of the top face of the cube are broken. However, these bond-breaking events never result in a planar structure or in a topomerization process because no simultaneous bond breaking is observed on the bottom face.

In contrast, a major rearrangement takes place during the simulation at 800 K. The bonding Li−C distances are reported in Figure 5 as a function of the simulation time. Under those conditions, four of the Li−C bonds lengthen within less than a picosecond to yield a planar aggregate. This point is especially remarkable as it indicates that the system readily escapes from the local minimum on the energy surface representing the cubic structure at this temperature.

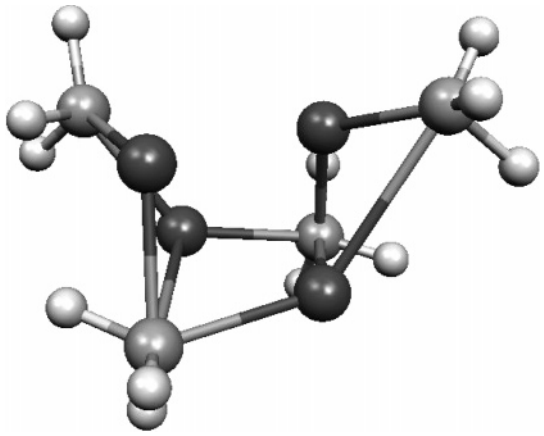

Figure 4. Snapshot at time $t = 5.2$ ps for cubic $(MeLi)_4$ at 600 K. Li−C bonds are plotted if shorter than 3.0 Å.

The process of this rearrangement is represented via the snapshots taken at 0.4, 0.6, and 0.8 fs (Figure 5). Opening of the aggregate takes place through a synchronous lengthening of the four Li−C bonds (as seen from the evolution of the four simultaneously increasing distances in Figure 5 around $t = 0.3$ ps). The resulting structure is a cube with sides alternatively opened (snapshot at 0.4 ps). Relaxation to the planar form then occurs, and the main motion observed is the shortening of long Li···C distances. This motion induces connections between Li and C atoms that were in trans arrangement in the initial cube.

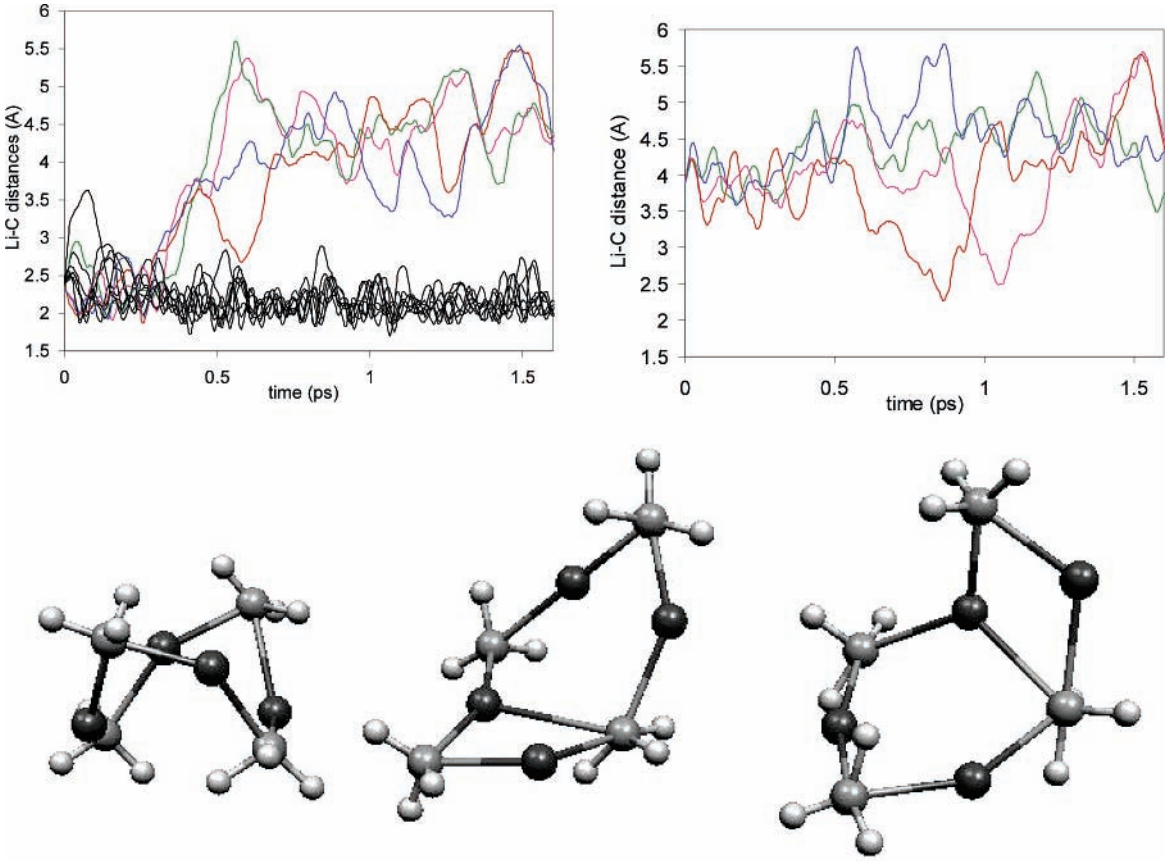

Figure 5. Bonding (top left) and nonbonding (top right) Li−C distances (in Å) as a function of the simulation time and snapshots at 0.4 (left bottom), 0.6 (center bottom), and 0.8 ps (right bottom) for the 800 K simulation on $(LiMe)_4$.

An example of such a shortening is given in a snapshot at 0.8 ps and can be also seen in Figure 5 (top, right) around $t = 1.0$ ps.

We next re-evaluate the inversion temperature for the reorganization of the cubic tetramer to the planar one. In the connection, the following procedure was used. A slow annealing was carried out starting at 100 K, with an annealing coefficient of 1.00005. Li−Li distances were monitored simultaneously with the running average of the temperature on a 0.3 ps time interval. A brutal rearrangement of the cubic structure to the planar one is observed for a temperature close to 650 K, which is consistent with the results of the constant temperature simulations. This value is larger than the value obtained within the static approach described above, but should be considered more accurate because it does not rely on the harmonic approximation for low-energy vibrational modes.

Conclusions

Car-Parrinello AIMD calculations were carried out to examine the effect of finite-temperature fluctuations on the structure of $(LiX)_n$ aggregates. It was found that the plane-wave basis/pseudopotential approach yields geometric and energetic results similar to those obtained with high-quality Gaussian basis sets. The AIMD indicates that the optimized minima are intrinsically stable at 300 K. Thus, the well-known dynamic behavior of the alkyllithium observed by NMR spectroscopy cannot be rendered by such short sampling. Considering global and local flexibility, our results indicate that the Li−X bond length is determined by the coordination number of the Li atoms, whereas the nonbonded X−X distances depend on the ability of the ligands to reach close-packed arrangements. The conformational behavior of the methyl moiety was also monitored. Even though free rotation of the CH_3 moiety is always observed, two different structural motions have been characterized. No conformational preference with respect to the Li skeleton can be found in the case of the dimer, whereas a preferred conformation was evidenced for the tetramer. The various topomers are nevertheless connected by low-energy barriers.

Important insight was obtained when comparing the behavior of the cubic and planar MeLi tetramers. Large fluctuations were observed for the planar tetramer, they induce a larger entropy contribution to the free energy, as supported by vibrational computations performed within the harmonic approximation. This entropic effect has been related to the isomerization of the cubic structure into the planar one within the simulation time at 800 K.

Although the calculations were performed in the gas phase, the results can probably be brought to bear on the behavior of comparable species in apolar noncoordinating solvents. Therefore, chemically relevant information seems within the reach of CP calculations. We showed that our data are directly related to structural analysis and that they are required preliminaries to a temperature-dependent study of reactivity. Applications of the AIMD technique to the analysis of spectroscopic (NMR) properties, of solvation patterns in organolithium chemistry, as well as reaction pathways toward electrophiles are currently under study.

Acknowledgment. Calculations have been performed on the IBM SP4 calculator at CRIHAN (Saint-Etienne-du-Rouvray, France), CINES (Montpellier, France), and IDRIS (Orsay, France). We acknowledge Dr. C. Giessner-Prettre for instigating this work and for dedicating continuous attention to its progress.

References and Notes

(1) Jones, R. O.; Lichtenstein, A. I.; Hutter, J. *J. Chem. Phys.* **1997**, *106*, 4566.

(2) Rousseau, R.; Marx, D. *Phys. Rev. Lett.* **1998**, *80*, 2574.

(3) Rousseau, R.; Marx, D. *J. Chem. Phys.* **1999**, *111*, 5091.

(4) Lyubartsev, A. P.; Laasonen, K.; Laaksonen, A. *J. Chem. Phys.* **2001**, *114*, 3120.

(5) Loeffler, H. H.; Mohammed, A. M.; Inada, Y.; Funahashi, S. *Chem. Phys. Lett.* **2003**, *379*, 452.

(6) Röthlisberger, U.; Klein, M. L. *J. Am. Chem. Soc.* **1995**, *117*, 42.

(7) Röthlisberger, U.; Sprik, M.; Klein, M. L. *J. Chem. Soc., Faraday Trans.* **1998**, *94*, 501.

(8) See, for instance: Brown, T. L.; Dickerhoof, D. W.; Bafus, D. A. *J. Am. Chem. Soc.* **1962**, *84*, 1371. Günther, H. *J. Braz. Chem. Soc.* **1999**, *10*, 241. Clayden, J. *Organolithiums: selectivity for synthesis*; Elsevier Science: Oxford (UK), 2002. Suzuki, M.; Koyama, H.; Noyori, R. *Bull. Chem. Soc. Jpn.* **2004**, *77*, 259.

(9) Chinn, J. W., Jr.; Lagow, R. J. *Organometallics* **1984**, *3*, 75.

(10) Bauer, W.; von Ragué Schleyer, P. *Adv. Carbanion Chem.* **1992**, *1*, 89 and references therein.

(11) Fraenkel, G.; Beckenbaugh, W. E.; Yang, P. P. *J. Am. Chem. Soc.* **1976**, *98*, 6878.

(12) Thomas, R. D.; Clarke, M. T.; Jensen, R. M.; Young, T. C. *Organometallics* **1986**, *5*, 1851.

(13) Heinzer, J.; Oth, J. F. M.; Seebach, D. *Helv. Chim. Acta* **1985**, *68*, 1848.

(14) Fraenkel, G.; Subramanian, S.; Chaow, A. *J. Am. Chem. Soc.* **1995**, *117*, 6300.

(15) Sikorski, W. H.; Reich, H. J. *J. Am. Chem. Soc.* **2001**, *123*, 6527.

(16) Reich, H. J.; Goldenberg, W. S.; Sanders, A. W.; Jantzi, K. L.; Tzschuche, C. C. *J. Am. Chem. Soc.* **2003**, *125*, 3509.

(17) McNeil, A. J.; Toombes, G. E. S.; Gruner, S. M.; Lobkovcky, E.; Collum, D. B.; Chandramouli, S. V.; Vanasse, B. J.; Ayers, T. A. *J. Am. Chem. Soc.* **2004**, *126*, 16559.

(18) Scott, R.; Granander, J.; Hilmersson, G. *J. Am. Chem. Soc.* **2004**, *126*, 6798.

(19) Jantsi, K. L.; Puckett, C. L.; Guzei, I. A.; Reich, H. J. *J. Org. Chem.* **2005**, *70*, 7520.

(20) Witanowski, W.; Roberts, J. D. *J. Am. Chem. Soc.* **1966**, *88*, 737.

(21) Clark, T.; Schleyer, P. v. R.; Pople, J. A. *J. Chem. Soc., Chem. Commun.* **1978**, 137.

(22) Haeffner, F.; Brandt, P.; Gawley, R. E. *Org. Lett.* **2002**, *4*, 2101.

(23) Ashweek, N. J.; Brandt, P.; Coldham, I.; Dufour, S.; Gawley, R. E.; Haeffner, F.; Klein, R.; Sanchez-Jimenez, G. *J. Am. Chem. Soc.* **2005**, *127*, 449.

(24) Kaufmann, E.; Raghavachari, K.; Reed, A. E.; Schleyer, P. von R. *Organometallics* **1988**, *7*, 1597.

(25) Kwon, O.; Sevin, F.; McKee, M. L. *J. Phys. Chem. A* **2001**, *105*, 913.

(26) Verstraete, P.; Deffieux, A.; Fritsch, A.; Rayez, J.-C.; Rayez, M.-T. *J. Mol. Struct. (THEOCHEM)* **2003**, *631*, 53.

(27) Breidung, J.; Thiel, W. *J. Mol. Struct.* **2001**, *599*, 239.

(28) Gohaud, N.; Begue, D.; Pouchan, C. *Chem. Phys.* **2005**, *310*, 85.

(29) Desjardins, S.; Flinois, K.; Oulyadi, H.; Davoust, D.; Giessner-Prettre, C.; Parisel, O.; Maddaluno, J. *Organometallics* **2003**, *22*, 4090.

(30) Fressigné, C.; Maddaluno, J.; Marquez, A.; Giessner-Prettre, C. *J. Org. Chem.* **2000**, *65*, 8899.

(31) Hæffner, F.; Brinck, T. *Organometallics* **2001**, *20*, 5134.

(32) Parisel, O.; Fressigné, C.; Maddaluno, J.; Giessner-Prettre, C. *J. Org. Chem.* **2003**, *68*, 1290.

(33) McGarrity, J. F.; Ogle, C. A. *J. Am. Chem. Soc.* **1985**, *107*, 1805−1810.

(34) McGarrity, J. F.; Ogle, C. A.; Brich, Z.; Loosli, H. R. *J. Am. Chem. Soc.* **1985**, *107*, 1810−1815.

(35) Weymeels, E.; Awad, H.; Bishoff, L.; Mongin, F.; Trécourt, F.; Quéguiner, G.; Marsais, F. *Tetrahedron* **2005**, *61*, 3245.

(36) Car, R.; Parrinello, M. *Phys. Rev. Lett.* **1985**, *55*, 2471.

(37) Frisch, M. J.; Trucks, G. W.; Schlegel, H. B.; Scuseria, G. E.; Robb, M. A.; Cheeseman, J. R.; Montgomery, J. A., Jr.; Vreven, T.; Kudin, K. N.; Burant, J. C.; Millam, J. M.; Iyengar, S. S.; Tomasi, J.; Barone, V.; Mennucci, B.; Cossi, M.; Scalmani, G.; Rega, N.; Petersson, G. A.; Nakatsuji, H.; Hada, M.; Ehara, M.; Toyota, K.; Fukuda, R.; Hasegawa, J.; Ishida, M.; Nakajima, T.; Honda, Y.; Kitao, O.; Nakai, H.; Klene, M.; Li, X.; Knox, J. E.; Hratchian, H. P.; Cross, J. B.; Adamo, C.; Jaramillo, J.; Gomperts, R.; Stratmann, R. E.; Yazyev, O.; Austin, A. J.; Cammi, R.; Pomelli, C.; Ochterski, J. W.; Ayala, P. Y.; Morokuma, K.; Voth, G. A.; Salvador, P.; Dannenberg, J. J.; Zakrzewski, V. G.; Dapprich, S.; Daniels, A. D.; Strain, M. C.; Farkas, O.; Malick, D. K.; Rabuck, A. D.; Raghavachari, K.; Foresman, J. B.; Ortiz, J. V.; Cui, Q.; Baboul, A. G.; Clifford, S.; Cioslowski, J.; Stefanov, B. B.; Liu, G.; Liashenko, A.; Piskorz, P.; Komaromi, I.; Martin, R. L.; Fox, D. J.; Keith, T.; Al-Laham, M. A.; Peng, C. Y.; Nanayakkara, A.; Challacombe, M.; Gill, P. M. W.; Johnson, B.; Chen, W.; Wong, M. W.; Gonzalez, C.; Pople, J. A. *Gaussian 03*, revision A.1; Gaussian, Inc.: Pittsburgh, PA, 2003.

(38) (a) Becke, A. D. *Phys. Rev.* **1988**, *A38*, 2155. (b) A. D. *J. Chem. Phys.* **1992**, *96*, 2155. (c) Lee, C.; Yang, W.; Parr, R. C. *Phys. Rev.* **1988**, *B37*, 785.

(39) (a) Perdew, J. P. *Phys. Rev.* **1986**, *B33*, 8822. (b) Becke, A. D. *J. Chem. Phys.* **1993**, *98*, 5648.

(40) Tuckerman, M. E.; Yarne, D. A.; Samuelson, S. O.; Hughes, A. L.; Martyna, G. J. *Comput. Phys. Commun.* **2000**, *128*, 333.

(41) Hartwigsen, C.; Goedecker, S.; Hutter, J. *Phys. Rev. B* **1998**, *58*, 3641.

(42) Troullier, N.; Martins, L. *Phys. Rev. B* **1991**, *43*, 1993.

(43) Martyna, G. J.; Tuckerman, M. E. *J. Chem. Phys.* **1999**, *110*, 2810.

(44) Martyna, G. J.; Tuckerman, M. E.; Klein, M. L. *J. Chem. Phys.* **1992**, *97*, 2635.

(45) Bickelhaupt, F. M.; van Eikema Hommes, N. J. R.; Fonseca Guerra, C.; Baerends, E. J. *Organometallics* **1996**, *15*, 2923.

(46) Wu, W.; McWeeny, R. *J. Mol. Struct. (THEOCHEM)* **1995**, *341*, 279.

(47) Fressigné, C.; Maddaluno, J.; Giessner-Prettre, C. *J. Chem. Soc., Perkin Trans. 2* **1999**, 2197.

(48) Ponec, R.; Roithová, J.; Gironés, X.; Lain, L.; Torre, A.; Bochicchio, R. *J. Phys. Chem. A* **2002**, *106*, 1019.

(49) Robinson, E. A.; Heard, G. L.; Gillespie, R. J. *J. Mol. Struct.* **1999**, *485−486*, 305.

(50) Rowsell, B. D.; Gillespie, R. J.; Heard, G. L. *Inorg. Chem.* **1999**, *38*, 4659.

(51) Andrews, L. *J. Chem. Phys.* **1967**, *47*, 4834.

(52) Grotjahn, D. B.; Pesch, T. C.; Xin, J.; Ziurys, L. M. *J. Am. Chem. Soc.* **1997**, *119*, 12368.

(53) Allen, M. D.; Pesch, T. C.; Robinson, J. S.; Apponi, A. J.; Grotjahn, D. B.; Ziurys, L. M. *Chem. Phys. Lett.* **1998**, *293*, 397.

(54) Grotjahn, D. B.; Pesch, T. C.; Brewster, M. A.; Ziurys, L. M. *J. Am. Chem. Soc.* **2000**, *122*, 4735.

(55) Weiss, E.; Lucken, E. A. C. *J. Organomet. Chem.* **1964**, *2*, 197.

(56) Weiss, E.; Hencken, G. *J. Organomet. Chem.* **1970**, *21*, 265.

(57) Arvidsson, P.; Ahlberg, P.; Hilmersson, G. *Chem. Eur. J.* **1999**, *5*, 1348.

(58) The temperature increase of 500 K corresponds roughly to the injection in the system of an extra energy amounting to a realistic 10 kcal mol^{-1}.

(59) (a) Aargaardt, O. M.; Meier, R. J.; Buda, F. *J. Am. Chem. Soc.* **1998**, *120*, 7174. (b) Hayes, R. L.; Fattal, E.; Govind, N.; Carter, E. A. *J. Am. Chem. Soc.* **2001**, *123*, 641.